

Magnetic properties of Fe/Co(001) superlattices from first-principles theoryAnders Bergman,¹ Till Burkert,² Biplab Sanyal,¹ Sonia Frota-Pessôa,³ Lars Nordström,¹ Andrei V. Ruban,⁴ Sergei I. Simak,² and Olle Eriksson^{1,*}¹*Department of Physics, Uppsala Universitet, Box 530, S-75121 Uppsala, Sweden*²*Department of Physics, Chemistry, and Biology, Linköping University, S-58183 Linköping, Sweden*³*Instituto de Física, Universidade de São Paulo, Caixa Postal 66318, 05315-970, São Paulo, SP, Brazil*⁴*Applied Materials Physics, Department of Materials and Engineering, Royal Institute of Technology (KTH), S-10044 Stockholm, Sweden*

(Received 29 March 2006; revised manuscript received 25 September 2006; published 8 November 2006)

The magnetic properties of Fe/Co(001) superlattices have been studied using fully-relativistic first-principles theories. The average magnetic moment shows a behavior similar to bulk Fe-Co alloys, i.e., an enhanced magnetic moment for low Co concentrations, as described by the Slater-Pauling curve. The maximum of the magnetization curve, however, is lowered and shifted towards the Fe-rich compositions. The increased average magnetic moment for the Fe-rich superlattices, compared to bulk Fe, is due to an enhancement of the Fe spin moment close to the Fe-Co interface. The orbital moments were found to be of the same size as in bulk. The effect of interface roughness on the magnetic properties was investigated, and it was found that—despite local fluctuations due to the varying coordination—the average magnetic moment is only slightly affected. From a mapping of first-principles interactions onto the screened generalized perturbation method, we calculate the temperatures for when Fe/Co superlattices break up into an alloy configuration. Furthermore, the tetragonal distortion of the superlattice structure was found to only have a minor effect on the magnetic moments. Also, the calculated easy axis of magnetization is in the film plane for all compositions studied. It lies along the [100] direction for Fe-rich superlattices and along the [110] direction for Co-rich compositions. The transition of the easy axis occurs around a Co concentration of 50%.

DOI: [10.1103/PhysRevB.74.174409](https://doi.org/10.1103/PhysRevB.74.174409)

PACS number(s): 75.70.Cn, 75.50.Bb, 75.30.Gw, 71.15.Mb

I. INTRODUCTION

Magnetic multilayers and superlattices have recently received much attention because of their technological importance in data storage and sensor applications as well as in fundamental research on magnetism.¹ The magnetic properties, e.g., the magnetic moments and the magnetic anisotropy, are affected by the presence of interfaces and the finite size of the layers. Deposition methods such as molecular beam epitaxy and sputter deposition techniques allow one to control the individual layer thicknesses on an atomic level, and in some cases phases that do not exist in bulk can be stabilized by pseudomorphic growth. An example of such a metastable phase is Co, which has an hcp structure in bulk, but can be stabilized in a bcc structure as a thin film on GaAs(110) (Ref. 2) and in Fe/Co superlattices on GaAs(110) (Refs. 3–5) and MgO(001).^{4–8} This allows one to study the influence of the structure, and thus the coordination, on the magnetic properties. In the following, we will limit the discussion to (001)-oriented superlattices, i.e., those that are grown on MgO(001).

Another reason for the interest in Fe/Co superlattices and multilayers is the unusual magnetic properties exhibited by bulk Fe-Co alloys,⁹ in particular their saturation magnetization that is described by the Slater-Pauling curve.^{9,10} The maximum average magnetic moment of $2.45\mu_B/\text{atom}$ is observed for a composition of $\approx 30\%$ Co. Early polarized neutron diffraction experiments have shown that this behavior is due to an enhancement of the Fe spin moment with increasing Co concentration.¹¹ The spin moment of Fe in these al-

loys increases from the bulk value to a maximum of about $3\mu_B/\text{atom}$ for 50% Co. The Co moment, on the other hand, remains virtually constant over the whole concentration range.

The magnetic properties of Fe/Co(001) superlattices have been characterized experimentally by different techniques.^{7,12–15} Even though these studies agree on the general trend of an enhanced Fe magnetic moment at the Fe-Co interface, there is a considerable discrepancy between some experimental findings. In a series of superconducting quantum interference device (SQUID) measurements, Blomqvist *et al.* found exceptionally high magnetic moments for a series of Fe/Co(001) superlattices that could not be explained by the expected enhancement of the Fe spin moment alone, and was attributed to an enhanced Co moment at the interface.⁷ More recent SQUID and x-ray circular magnetic dichroism (XMCD) studies on similar samples, however, did not reproduce such high values for the magnetic moment.¹⁴

These experimental discrepancies call for a more thorough investigation, and in this work we present a first-principles study of the magnetic properties of Fe/Co(001) superlattices. We have calculated the magnetic profile for a wide range of superlattice compositions and individual layer thicknesses. The magnetic profile at the Fe-Co interface was previously studied by Niklasson *et al.*,¹⁶ and a first-principles study of the magnetic properties of Fe/Co multilayers was communicated in Ref. 17. In the present work, we also study the effect of interface roughness, which is known to have a strong effect on the magnetic properties of multilayers,^{18,19} as well as the effect of the structural distortion from the

cubic symmetry that is caused by the lattice mismatch of the constituent atoms. In addition, we investigated the magnetic anisotropy for some superlattice compositions.

II. CALCULATIONAL DETAILS

The calculations presented here were done using three different electronic structure methods that are based on the density functional theory. The spin and orbital moments of the Fe/Co(001) superlattices were calculated with the real-space linear muffin-tin orbital method in the atomic sphere approximation (RS-LMTO-ASA).^{20,21} The RS-LMTO-ASA method is a self-consistent method that is similar to the ordinary reciprocal-space LMTO-ASA method,²² except that the eigenvalue problem is solved by using the recursion method in real space to obtain the local density of states from the continued fraction expansion of Green's function matrix elements.²³ In the present calculations, the continued fraction in the recursion method is terminated after 25 recursion steps with the Beer-Pettifor terminator.²⁴ For the exchange-correlation functional the local spin density approximation was used.²⁵ The spin-orbit interaction is treated at each variational step with the orbital polarization²⁶ included.

The RS-LMTO-ASA method does not need periodic boundary conditions, and is thus well suited to investigate impurities and other defects in metals. Therefore, the method was used in this work to study the influence of interface roughness on the local magnetic properties. For these impurity-like calculations the electronic structure of the unperturbed host, in this case an Fe₆/Co₂(001) superlattice, is first calculated self-consistently. Then an impurity atom is embedded as a local perturbation in the host. The atoms in a small region surrounding the impurity are then recalculated until self-consistency is reached. This region is chosen so that the charge and magnetization densities of the outermost atoms differ insignificantly from the unperturbed atoms. A more detailed description of the embedding of impurities can be found in Ref. 27.

To investigate the effect of the tetragonal distortion from the cubic structure on the magnetic properties, we performed a structural optimization for some of the superlattice compositions using the VASP (Refs. 28 and 29) plane wave code within the projector augmented wave method.³⁰ A kinetic energy cutoff of 500 eV was used for the plane waves included in the basis set, and the exchange-correlation potential was treated in the generalized gradient approximation. The Hellmann-Feynman forces were calculated with a tolerance of 0.02 eV/Å. For the Brillouin zone integration an $8 \times 8 \times 2$ special k -point grid was used.³¹

The calculations of the magnetocrystalline anisotropy energies (MAE) were done with a fully-relativistic implementation of the full-potential linear muffin-tin orbital (FP-LMTO) method.³² The scalar-relativistic corrections were included in the calculation of the radial basis functions inside the muffin-tin spheres, whereas the spin-orbit coupling was included at the variational step. For the exchange-correlation potential the local density approximation (LDA) was used. The MAE was evaluated with the force theorem, i.e., as the difference of the eigenvalue sums for the two magnetization

directions. The accuracy of this approach has been tested several times and found to yield acceptably accurate values (see, e.g., Ref. 33). In this approach the electron density was first calculated self-consistently with a scalar-relativistic Hamiltonian using the point-group symmetries that are common to both magnetization directions. Then, in a subsequent step, the eigenvalues were obtained by a single diagonalization for each magnetization direction, using the fully relativistic Hamiltonian and the scalar-relativistic self-consistent potential. The calculation of the self-consistent potential was done with a $20 \times 20 \times 5$ k -point mesh, and for the force theorem calculations a $64 \times 64 \times 16$ k -point mesh was used. For the evaluation of the eigenvalue sums the modified tetrahedron method (MTM) was employed.³⁴ The procedure is different from that of Ref. 17, where the calculations were done using the Gaussian broadening method³¹ (GBM) for the evaluation of the eigenvalue sum. The advantage with the MTM is that it is exact in the limit of an infinite number of k points. The GBM, on the other hand, may smear out details of the Fermi surface and lead to a less accurate Fermi energy.³¹

III. RESULTS

A. Magnetic moments

The spin and orbital moments of Fe_{*n*}/Co_{*m*}(001) superlattices were calculated with the RS-LMTO-ASA method for a wide range of compositions. The indices n and m denote the number of atomic layers of Fe and Co, respectively. For these calculations the crystal structure of the superlattices was assumed to be body-centered cubic (bcc), using a lattice parameter interpolated between bulk bcc Fe and bcc Co² according to Vegard's law.

The calculated spin and total moments are presented in Fig. 1 as a function of the Co concentration. For clarity, only the data sets for $n+m=4$ and 8 are presented here. The superlattices show a behavior that is similar to that of the magnetic moment of bulk Fe-Co alloys, i.e., with an increase of both the spin and the total magnetic moment for small Co concentrations.^{10,11,35} However, the enhancement of the total magnetic moment is less pronounced for the superlattices compared to the bulk data. With an increasing thickness of the layers the maximum magnetic moment decreases and is shifted toward lower Co concentrations. The calculated total magnetic moments agree well in general with recent SQUID measurements,¹⁴ whereas the high moments found in earlier SQUID measurements⁷ are not reproduced.

The experimental point at 40% Co concentration from Ref. 14 does however deviate substantially from the theoretical curve, and in addition seems to deviate from the general trend of the experimental data points of Ref. 14. For a closer look at the effect of the layer thickness on the magnetic moment, we show in Fig. 2 the total magnetic moment of superlattices with a Co concentration of 50% and $n=m=1-6$. It can be seen that, for equal concentration, superlattices with thinner layers have higher magnetic moments than those with thicker layers. The increase of the magnetic moment with decreasing layer thickness indicates that the enhancement of the moments is larger in the interface region

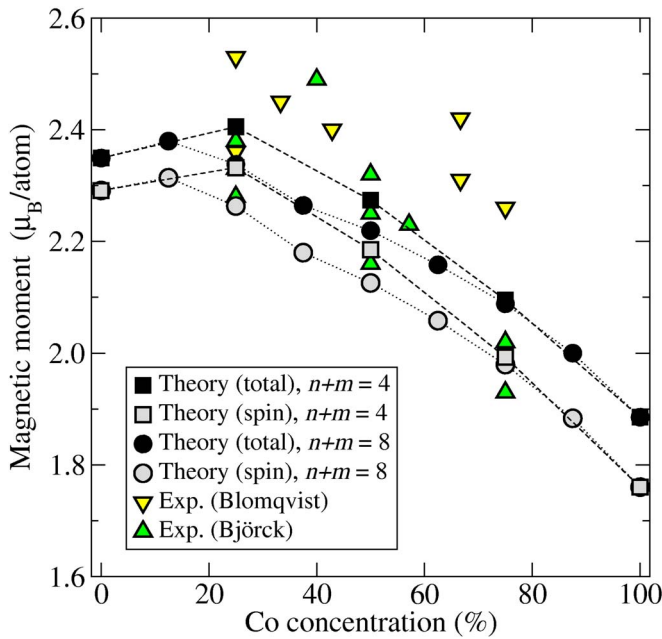


FIG. 1. (Color online) Spin and total magnetic moments for bcc $\text{Fe}_n/\text{Co}_m(001)$ superlattices, for $n+m=4$ and 8, as a function of the Co concentration, calculated with the RS-LMTO-ASA method. The experimental total moments are from Refs. 7 and 14.

than in the middle of the layers, where a more bulklike surrounding is present. To investigate the enhancement of the magnetic moments, the local spin moments for the individual layers in the Fe_6/Co_2 , Fe_4/Co_4 , and Fe_2/Co_6 superlattices are shown in Fig. 3. From this figure, it is clearly seen that the Fe spin moments at the interface are enhanced, up to a value of $2.6\mu_B$, whereas all other Fe atoms exhibit almost bulklike values. Since the Fe atoms at the interface are the ones having Co atoms as nearest neighbors, it is clear that the enhancement is due to the surrounding Co atoms. The interface Fe atoms have the same number of Co neighbors for all superlattices, and the enhancement of the spin moments is therefore almost identical in magnitude, independent of the layer thickness.

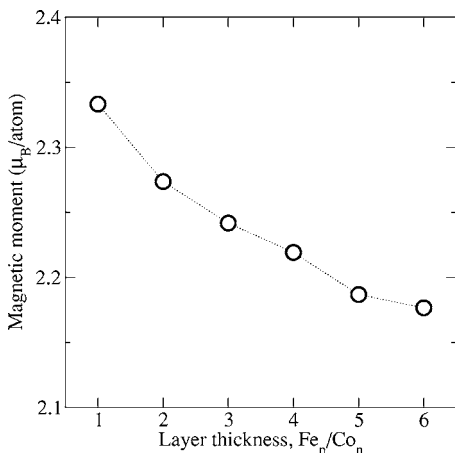


FIG. 2. Average magnetic moments for bcc $\text{Fe}_n/\text{Co}_n(001)$ superlattices with $n=1-6$, calculated with the RS-LMTO-ASA method.

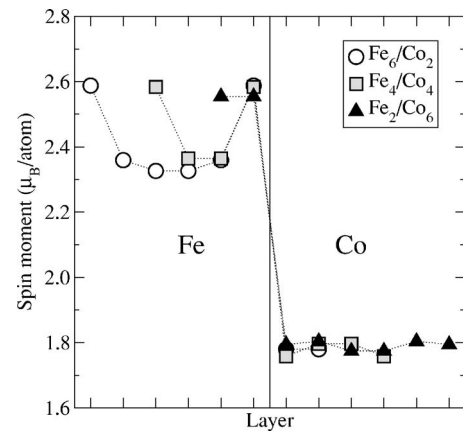


FIG. 3. Local spin magnetic moments for three superlattice compositions, calculated with the RS-LMTO-ASA method. The vertical line indicates the Fe/Co interface.

This short-ranged enhancement of the Fe spin moment is limited to the interface layer and is consistent with other theoretical studies of Fe-Co interfaces.^{16,36-40} The spin moment of the Co atoms, on the other hand, remains constant regardless of the position in the superlattice and of the proximity to Fe atoms. The trend of a constant Co moment agrees with the experimentally found behavior of bulk Fe-Co alloys¹¹ and Fe/Co(001) superlattices.¹⁴ The enhancement of the spin moments of the Fe atoms is also consistent with experimental findings, although the calculated enhancement is smaller than what is found experimentally.¹⁴ The enhanced spin moments of the Fe atoms can be explained by hybridization effects between the Fe atoms and neighboring Co atoms.^{36,37}

The calculated orbital moments for the Fe_6/Co_2 , Fe_4/Co_4 , and Fe_2/Co_6 superlattices are shown in Fig. 4. As opposed to the behavior of the spin moment, the orbital moment for the interface Co atoms decreases by almost 30%, whereas the orbital moments for the other atoms only vary slightly between different sites in the superlattice. The calculated Co orbital moments reproduce the experimentally observed val-

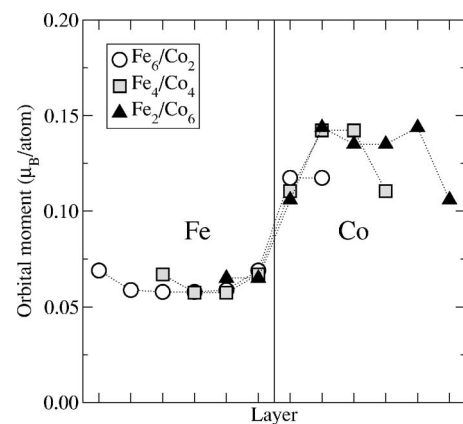


FIG. 4. Orbital moments as a function of the position in the superlattice for three different superlattice compositions, calculated with the RS-LMTO-ASA method. The vertical line indicates the Fe/Co interface.

ues with rather good accuracy, whereas the calculated Fe orbital moments are too small.¹⁴ This discrepancy is most likely due to the fact that the real-space method, like the reciprocal-space LMTO,⁴¹ slightly underestimates the orbital moments compared to experimental data, as well as an uncertainty in the determination of the experimental orbital moments from the XMCD sum rules.

B. Interdiffusion simulations

Diffusion at the interfaces is known to strongly affect the magnetic properties of superlattices.¹⁸ Experimentally, however, the morphology of the interface in Fe/Co superlattices is still a matter of debate, but is known to be dependent on temperature.^{5,8,12} To address this issue we have performed standard Monte Carlo simulations with concentration dependent effective interactions extracted from first-principles calculations in the framework of the screened generalized perturbation method (SGPM).⁴² We took into account the local character of diffusion at low temperatures and approximated the temperature induced intermixing of Fe/Co layers by the destruction of the local $B2$ -type symmetry at the Fe-Co interface.⁴³ Fe_6/Co_2 and Fe_2/Co_6 systems were considered and the temperature for a transition from a $B2$ structure to a disordered state was estimated through standard specific heat calculations with two sets of effective interactions, one corresponding to the overall Fe and Co concentrations in the system and the other corresponding to the $B2$ -type local symmetry, i.e., $\text{Fe}_{50}/\text{Co}_{50}$. The results for these two sets provide obvious limiting points for the region of temperatures at which the destruction of the local $B2$ -type symmetry and therefore the initial interdiffusion is expected to occur.

Our results are presented in Fig. 5 and show that the transition temperature is higher for Fe_6Co_2 compared to Fe_2Co_6 . They also indicate that the temperature at which the samples are prepared can strongly affect the degree of Fe-Co interdiffusion. Remarkably, higher Co content in the sample facilitates Fe-Co interdiffusion leading to a lower temperature needed to destroy the ideal structure with Fe and Co atoms occupying only their respective layers. In particular, in the Fe_2/Co_6 multilayer system interdiffusion is expected at temperatures higher than ≈ 520 – 610 K [Fig. 5(a)] and in Fe_6/Co_2 at temperatures higher than ≈ 660 – 950 K [Fig. 5(b)]. These simple estimates turn out to be in good agreement with experimental temperatures for when interdiffusion is initiated: 623 – 673 K for Fe_2/Co_6 and 773 – 823 K for Fe_6/Co_2 , respectively.⁴⁴

C. Interdiffusion effects

In order to examine the influence of interface roughness on the magnetic moments of Fe/Co superlattices, we have performed calculations for Fe_6/Co_2 corresponding to 25% and 50% intermixing of the interfacial layers. However, the differences in the average magnetic moments for these systems were not significant. Compared to the total moment for the perfect Fe_6/Co_2 superlattice, $2.34\mu_B$, the moments for the interdiffused systems were found to be $2.33\mu_B$ for both 25% and 50% interdiffusion.

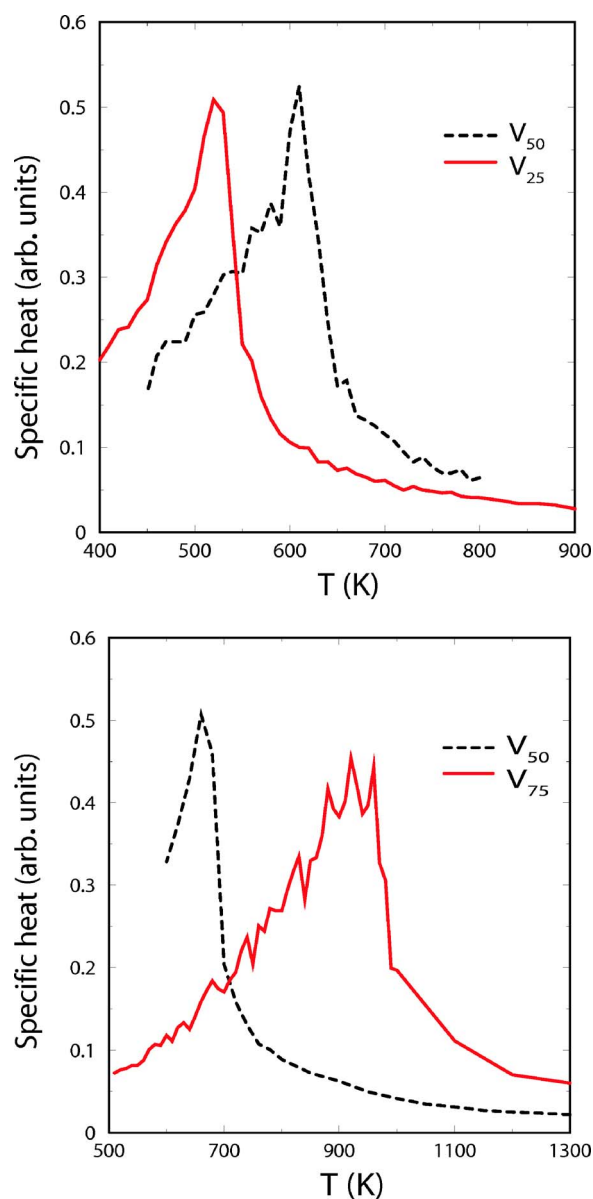


FIG. 5. (Color online) Calculated specific heat for (a) Fe_2Co_6 and (b) Fe_6Co_2 multilayers as a function of temperature. Parameters in the SGPM method were calculated from a $\text{Fe}_{0.5}\text{Co}_{0.5}$ alloy (dashed line), a $\text{Fe}_{0.25}\text{Co}_{0.75}$ alloy [solid line, panel (a)], and a $\text{Fe}_{0.75}\text{Co}_{0.25}$ alloy [solid line, panel (b)].

An investigation of the local magnetic structure around interdiffused atoms was performed by considering single impurities at the Fe-Co interface for an Fe_6/Co_2 superlattice. The two configurations considered in this study were an Fe atom placed at a Co interface site, which is illustrated in Fig. 6(b), and a Co atom placed on an Fe interface site, as shown in Fig. 6(c). For an Fe atom occupying a Co site, a very small increase, from $2.58\mu_B$ to $2.62\mu_B$, of the Fe spin moment is observed. This increase can be explained by the difference in coordination between a site on the Fe side of the interface, which has four nearest and one next-nearest Co neighbor, and on the Co side, which has four nearest and five next-nearest Co neighbors. On the other hand, an Fe atom on a Co site decreases the spin moment for the surrounding Fe

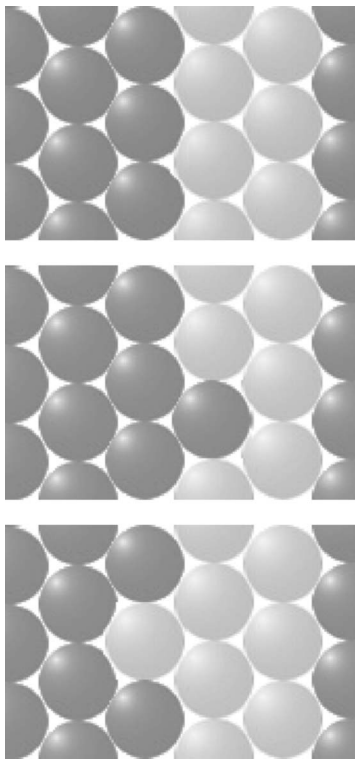


FIG. 6. Illustration of single impurities at the Fe-Co interface. The upper panel shows a perfect interface. The center panel shows an Fe atom at an Co site, whereas the lower panel shows a Co atom at an Fe site.

atoms in the interface layer, from $2.58\mu_B$ to $2.53\mu_B$, so that the net effect is actually a decrease of the average magnetic moment. When a Co atom is placed at an interface Fe site, the spin moment of the Co atom does not change. The Fe atoms surrounding the impurity Co atom do however increase their spin moments, from $2.36\mu_B$ for a perfect interface to $2.43\mu_B$ due to the increased Co coordination number.

D. Structural distortion

So far only bcc Fe/Co(001) superlattices have been discussed. The difference of the equilibrium lattice parameters of bulk bcc Fe and bcc Co² amounts to only 1.6%, and thus the tetragonal distortion of the individual Fe and Co layers from a bcc structure are expected to be small. To examine the influence of these distortions on the magnetic properties, we performed a structural optimization for some superlattice compositions, namely Fe₆/Co₂, Fe₄/Co₄, and Fe₂/Co₆. The relaxed structures were found to differ very little from the perfect bcc superlattice, resulting in a tetragonal distortion with an increase of $\approx 1\%$ of the out-of-plane lattice parameter and a volume change of less than 1.5%. It was found that the small distortion from a cubic symmetry only has a minor effect on the magnetic moments. A comparison between the cubic and the relaxed Fe₄/Co₄ superlattice shows a 1% decrease of the spin moment for the latter. The orbital moment is decreased by 4% for the relaxed superlattice. The effect of these distortions on the magnetic anisotropy will be discussed in the next section.

TABLE I. Calculated magnetocrystalline anisotropy energies, in $\mu\text{eV}/\text{atom}$, for the relaxed Fe₆/Co₂, Fe₄/Co₄, and Fe₂/Co₆ superlattices, obtained with the FP-LMTO method. The experimental values are from Ref. 7.

	$E^{110} - E^{100}$		$E^{100} - E^{001}$
	Calc.	Expt.	Calc.
Fe ₆ /Co ₂	4.5	0.4	-42
Fe ₄ /Co ₄	≈ 0		-46
Fe ₂ /Co ₆	-2.6	-1.0	-58

E. Magnetic anisotropy

The MAE was calculated for the relaxed Fe₆/Co₂, Fe₄/Co₄, and Fe₂/Co₆ superlattices, since it is strongly dependent on the c/a ratio of the layers.^{45,46} The out-of-plane MAE, which is defined as $E^{100} - E^{001}$, where E^{nmk} is the total energy with the magnetization aligned along the direction $[nmk]$, is presented in Table I. Note that the calculated values are merely the magnetocrystalline anisotropy, i.e., the intrinsic contribution resulting from the spin-orbit interaction, which is negative for the studied compositions, and hence results in an easy axis of magnetization that lies in the plane of the film. In thin magnetic films and multilayers, the so-called shape anisotropy that originates from the mutual dipole interaction of the magnetic moments makes a significant contribution to the total MAE. It always favors an orientation of the easy axis of magnetization in the film plane. In the present case, both contributions to the MAE favor an in-plane easy axis. The effective MAE, which is measured experimentally, can be calculated from $K_{\text{eff}} = K_{\text{MCA}} - \mu_0 M_s^2 / 2$, where M_s is the saturation magnetization.⁴⁷ The shape anisotropy in Fe/Co(001) superlattices is of the order of $150 \mu\text{eV}/\text{atom}$. For the compositions studied here, the magnitude of the out-of-plane MAE increases with the Co concentration, as can be seen from Table I.

The in-plane MAE, which is defined as $E^{110} - E^{100}$, is much smaller than the out-of-plane MAE, owing to the square symmetry within the plane of the sample. The results for the calculated in-plane MAE are given in Table I, together with the experimentally obtained values from Ref. 7. The agreement between the calculated values and the measured values is satisfactory, considering the tiny energy differences of the order of μeV that have to be resolved. Experimentally, the transition from the [100] easy axis to the [110] easy axis with increasing Co concentration is found to occur around 33% Co,⁷ whereas the crossover occurs at about 50% for the calculated values. It is interesting to note that a crossover from the [100] to the [111] direction for the easy axis occurs in bulk bcc Fe-Co alloys at a Co concentration of 45%.⁹ Thus it appears that the behavior of the in-plane MAE of Fe/Co(001) superlattices is similar to that of bulk Fe-Co alloys, if one considers the fact that the easy axis of magnetization is forced into the plane by the shape anisotropy. That is, for Co-rich superlattices the easy axis is along [110], which is the projection of [111] onto the plane of the film.

We attempted to separate the effect on the out-of-plane MAE due to the deviation from the cubic symmetry owing to the tetragonal distortion of the lattice on the one hand, and the chemical modulation along the growth direction on the other hand. To accomplish this, the atomic positions of the relaxed structures for the superlattices considered above were used to model a random Fe-Co alloy of the respective composition. The alloy was treated within the virtual crystal approximation, which is expected to work well in the case of Fe and Co.⁴⁸ The calculated values for the out-of-plane MAE of these hypothetical superlattices are of the order of 10 $\mu\text{eV}/\text{atom}$, i.e., with a reversed sign compared to the values reported in Table I. The trend of an increasing magnitude of the MAE with increasing Co concentration, however, is preserved. In addition, we calculated the out-of-plane MAE for a bcc Fe_4/Co_4 superlattice, i.e., without lattice distortions, and it was found to be only 5% larger than that of the relaxed superlattice. From this simple calculation it can be concluded that it is the chemical modulation along the growth direction, i.e., an interface contribution, that dominates the out-of-plane MAE. It should be noted that the chemical modulation breaks the cubic symmetry and results in a tetragonal symmetry, even if an ideal bcc structure is assumed. It is for this reason a tetragonal lattice distortion of the multilayers only marginally affects the calculated MAE.

IV. SUMMARY

The magnetic moments and the magnetic anisotropy energy of Fe/Co(001) superlattices were calculated from first principles. The concentration dependence of the magnetic moment is similar to what is observed in bulk Fe-Co alloys, which is described by the Slater-Pauling curve. The maximum saturation moment, however, is less pronounced and shifted toward lower Co concentrations. The enhancement of the magnetic moments for Fe-rich superlattices is traced to an enhanced Fe spin moment close to the Fe-Co interface. No evidence for an increased Co magnetic moment was

found. The orbital moments are of the same size as in bulk, with a small increase for interface Fe atoms, while the Co atoms at the interface have slightly decreased orbital moments. The calculated total magnetic moments agree well with a recent experimental study.¹⁴

The effect of interface roughness was investigated, and the average magnetic moments were found to be virtually unaffected, despite local fluctuations due to the varying coordination. From an analysis based on SGPM we calculate the temperatures for when ideal multilayers break up into an alloy. The Fe_2Co_6 multilayer is found to transform into an alloy at ~ 550 K and the Fe_6Co_2 multilayer at ~ 800 K, in qualitative agreement with experiments. Using relaxed superlattice structures, the effect of tetragonal distortions on the magnetic properties was investigated. The influence of the distortion on the magnetic moments was found to be small.

Fe-rich superlattices favor an easy axis along the [100] direction, whereas the Co-rich systems have the easy axis along the [110] direction, in agreement with experimental findings. The transition of the easy axis occurs around a Co concentration of 50%. The in-plane easy axis of magnetization is due to two contributions: The chemical modulation that breaks the cubic symmetry and the shape anisotropy.

ACKNOWLEDGMENTS

This work was carried out with financial support from the Swedish Research Council (VR), the Göran Gustafsson foundation, the Foundation for Strategic Research (SSF), Conselho Nacional de Pesquisas, Brazil (CNPq), and from Seagate Technology, Bloomington. We gratefully acknowledge John M. Wills for supplying the FP-LMTO code. Parts of the calculations were performed at the Swedish National Supercomputer Center (NSC) and the High Performance Computing Center North (HPC2N). We gratefully acknowledge Matts Björck and Gabriella Andersson for fruitful discussions.

*Electronic address: Olle.Eriksson@fysik.uu.se

¹ *Ultrathin Magnetic Structures*, edited by J. A. C. Bland and B. Heinrich (Springer, New York, 1994), Vol. 1.

² G. A. Prinz, *Phys. Rev. Lett.* **54**, 1051 (1985).

³ B. Swinnen, J. Dekoster, J. Meersschaut, S. Demuyne, S. Cottener, G. Langouche, and M. Rots, *J. Magn. Magn. Mater.* **175**, 23 (1997).

⁴ J. Dekoster, E. Jedryka, C. Mény, and G. Langouche, *J. Magn. Magn. Mater.* **121**, 69 (1993).

⁵ J. P. Jay, E. Jedryka, M. Wójcik, J. Dekoster, G. Langouche, and P. Panissod, *Z. Phys. B: Condens. Matter* **101**, 329 (1996).

⁶ J. Dekoster, E. Jedryka, M. Wójcik, and G. Langouche, *J. Magn. Magn. Mater.* **126**, 12 (1993).

⁷ P. Blomqvist, R. Wäppling, A. Broddefalk, P. Nordblad, S. G. E. te Velthuis, and G. P. Felcher, *J. Magn. Magn. Mater.* **248**, 75 (2002).

⁸ P. Blomqvist and R. Wäppling, *J. Cryst. Growth* **252**, 120 (2003).

⁹ D. Bonnenberg, K. A. Hempel, and H. P. J. Wijn, in *Magnetic Properties of 3d, 4d and 5d Elements, Alloys and Compounds*, edited by H. P. J. Wijn, Landolt-Börnstein: Numerical Data and Functional Relationships in Science and Technology, New Series, Group III: Crystal and Solid State Physics, Vol. 19, Pt. a (Springer-Verlag, Berlin, 1986).

¹⁰ R. M. Bozorth, *Ferromagnetism* (Van Nostrand, New York, 1951).

¹¹ M. F. Collins and J. B. Forsyth, *Philos. Mag.* **8**, 401 (1963).

¹² B. Kalska, P. Blomqvist, L. Häggström, and R. Wäppling, *J. Phys.: Condens. Matter* **13**, 2963 (2001).

¹³ L. Häggström, B. Kalska, E. Nordström, P. Blomqvist, and R. Wäppling, *J. Alloys Compd.* **347**, 252 (2002).

¹⁴ M. Björck, G. Andersson, B. Lindgren, R. Wäppling, V. Stanciu, and P. Nordblad, *J. Magn. Magn. Mater.* **284**, 273 (2004).

¹⁵ S. Kamali-M, A. Bergman, G. Andersson, V. Stanciu, and L. Häggström, *J. Phys.: Condens. Matter* **18**, 5807 (2006).

- ¹⁶A. M. N. Niklasson, B. Johansson, and H. L. Skriver, Phys. Rev. B **59**, 6373 (1999).
- ¹⁷O. Eriksson, L. Bergqvist, E. Holmström, A. Bergman, O. Le Bacq, S. Frota-Pessôa, B. Hjörvarsson, and L. Nordström, J. Phys.: Condens. Matter **15**, S599 (2003).
- ¹⁸E. Holmström, L. Nordström, L. Bergqvist, B. Skubic, B. Hjörvarsson, I. A. Abrikosov, P. Svedlindh, and O. Eriksson, Proc. Natl. Acad. Sci. U.S.A. **101**, 4742 (2004).
- ¹⁹S. Frota-Pessôa, A. B. Klautau, and S. B. Legoas, Phys. Rev. B **66**, 132416 (2002).
- ²⁰S. Frota-Pessôa, Phys. Rev. B **46**, 14570 (1992).
- ²¹S. Frota-Pessôa, Phys. Rev. B **69**, 104401 (2004).
- ²²H. L. Skriver, *The LMTO Method: Muffin-Tin Orbitals and Electronic Structure* (Springer, Berlin, 1984).
- ²³R. Haydock, *Solid State Physics* (Academic, New York, 1980), Vol. 35, p. 216.
- ²⁴N. Beer and D. Pettifor, *The Electronic Structure of Complex Systems* (Plenum, New York, 1984).
- ²⁵U. von Barth and L. Hedin, J. Phys. C **5**, 1629 (1972).
- ²⁶O. Eriksson, M. S. S. Brooks, and B. Johansson, Phys. Rev. B **41**, R7311 (1990).
- ²⁷S. B. Legoas and S. Frota-Pessôa, Phys. Rev. B **61**, 12566 (2000).
- ²⁸G. Kresse and J. Hafner, Phys. Rev. B **47**, R558 (1993).
- ²⁹G. Kresse and J. Furthmüller, Phys. Rev. B **54**, 11169 (1996).
- ³⁰P. E. Blöchl, Phys. Rev. B **50**, 17953 (1994).
- ³¹H. J. Monkhorst and J. D. Pack, Phys. Rev. B **13**, 5188 (1976).
- ³²J. M. Wills, O. Eriksson, M. Alouani, and D. L. Price, in *Electronic Structure and Physical Properties of Solids: The Uses of the LMTO Method* (Springer, Berlin, 2000), pp. 148–167.
- ³³O. Eriksson, in *Band Ferromagnetism, Ground State and Finite Temperature Phenomena*, edited by K. Baberschke, M. Donath, and W. Nolting (Springer, Berlin, 2001), p. 243.
- ³⁴P. E. Blöchl, O. Jepsen, and O. K. Andersen, Phys. Rev. B **49**, 16223 (1994).
- ³⁵J. M. MacLaren, T. C. Schulthess, W. H. Butler, R. Sutton, and M. McHenry, J. Appl. Phys. **85**, 4833 (1999).
- ³⁶A. Bergman, E. Holmström, A. M. N. Niklasson, L. Nordström, S. Frota-Pessôa, and O. Eriksson, Phys. Rev. B **70**, 174446 (2004).
- ³⁷P. Mohn, *Magnetism in the Solid State: An Introduction* (Springer, New York, 2003).
- ³⁸J. Kübler, *Theory of Itinerant Magnetism* (Oxford Science Publications, Clarendon Press, New York, 2000).
- ³⁹I. Turek, J. Kudrnovsky, V. Drchal, and P. Weinberger, Phys. Rev. B **49**, 3352 (1997).
- ⁴⁰P. James, O. Eriksson, B. Johansson, and I. A. Abrikosov, Phys. Rev. B **59**, 419 (1999).
- ⁴¹O. Eriksson, B. Johansson, R. C. Albers, A. M. Boring, and M. S. Brooks, Phys. Rev. B **42**, R2707 (1990).
- ⁴²A. V. Ruban, S. Shallcross, S. I. Simak, and H. L. Skriver, Phys. Rev. B **70**, 125115 (2004).
- ⁴³Note that an accurate approach here would be the kinetic Monte Carlo simulation, which in this particular case is rather cumbersome.
- ⁴⁴P. Blomqvist and R. Wäppling, J. Cryst. Growth **252**, 120 (2003).
- ⁴⁵O. Hjortstam, K. Baberschke, J. M. Wills, B. Johansson, and O. Eriksson, Phys. Rev. B **55**, 15026 (1997).
- ⁴⁶T. Burkert, O. Eriksson, P. James, S. I. Simak, B. Johansson, and L. Nordström, Phys. Rev. B **69**, 104426 (2004).
- ⁴⁷M. T. Johnson, P. J. H. Bloemen, F. J. A. den Broeder, and J. J. de Vries, Rep. Prog. Phys. **59**, 1409 (1996).
- ⁴⁸P. James, O. Eriksson, O. Hjortstam, B. Johansson, and L. Nordström, Appl. Phys. Lett. **76**, 915 (2000).